Integration of a Storage Device to the DC Bus of a Grid-Forming Controlled HVDC Interconnection

5 authors, including:

Ebrahim Rokrok
SiemensEnergy
17 PUBLICATIONS   **182** CITATIONS

Qoria Taoufik
Maschinenfabrik Reinhausen
35 PUBLICATIONS   **365** CITATIONS

Xavier Guillaud
École Centrale de Lille
219 PUBLICATIONS   **3,478** CITATIONS

Antoine Bruyere
École Centrale de Lille
35 PUBLICATIONS   **430** CITATIONS

Some of the authors of this publication are also working on these related projects:

Project   Model based design of power electronic devices with guaranteed parameters View project

Project   Master Thesis View project

Integration of a Storage Device to the DC Bus of a Grid-Forming Controlled HVDC Interconnection

Ebrahim Rokrok
Antoine Bruyere
Bruno Francois
Xavier Guillaud
L2EP, Univ. Lille, Arts et Metiers Institute of Technology,
Centrale Lille, Yncrea Hauts-de-France,
ULR 2697 - L2EP - Laboratoire d'Electrotechnique
et d'Electronique de Puissance, F-59000
Lille, France
ebrahim.rokrok@centralelille.fr

Taoufik Qoria
Maschinenfabrik Reinhausen, EAP department, 93059
Regensburg, Germany
t.qoria@reinhausen.com

Abstract—This paper assesses the performance of a high-voltage direct-current (HVDC) interconnection for providing virtual inertia to the power system. The impact of inertia provision on the DC bus dynamics and system frequency when one or both converter terminals are controlled with a virtual synchronous machine (VSM) based grid-forming strategy is evaluated. It has been demonstrated that an identical inertial support cannot be provided to both terminals due to a fundamental conflict between the DC voltage control and inertia emulation tasks. Therefore, it has been proposed to integrate a storage device (e.g. flywheel energy storage system (FESS)) with an additional converter to the DC link in order to control the DC voltage. Doing so, the DC voltage control is not couple with the inertia emulation at each substation and the obtained results have shown that a good performance in the DC voltage control as well as a proper inertia support provision are achieved. Finally, a discussion on a simplified approach to size the storage system is presented.

Index Terms—Flywheel energy storage system, grid-forming control, HVDC interconnection, virtual inertia.

I. INTRODUCTION

The integration of large-scale renewable power generation with power electronic interfaces into power systems is leading to reduce equivalent inertia and rising the levels of rate-of-change-of frequency (RoCoF) in response to the grid disturbances [1]. In such condition, the high voltage direct current (HVDC) system's control for providing virtual inertia could be an effective measure for increasing the power system equivalent inertia and improving the frequency dynamics.

Several publications have proposed to utilize voltage source converter (VSC) HVDC systems for providing virtual inertia. Many of the proposed control methods are based on the grid-following control concept, where they use the frequency derivative (i.e. df/dt or RoCoF) to synthetize the inertial response. Such strategies can be easily integrated with conventional VSC control loops but they rely on a phase-locked loop

(PLL) for the synchronization with the grid and to estimate the df/dt. However, under weak grid condition, in addition to difficulties with estimating effectively the df/dt, some stability issues are reported in the literature [2], [3].

To tackle these challenges, the control system of the power converters at HVDC substations has to be changed from grid-following control to grid-forming control in which the converters behave as a voltage source. Various grid-forming control strategies with inherent ability of inertia emulation (e.g. droop control [4], virtual synchronous machine (VSM) [5], power synchronization based with PI controller [6], Synchronverters [7], etc.) that do not rely on a PLL to be synchronized with the grid have been widely studied in the literature. Most of the previous publications on grid-forming control for HVDC applications have studied the implementation and control system performance for an individual converter terminal [8], [9].

The use of a grid forming control in an HVDC converter is interesting for the grid to which it is connected due to the inertial effect that can be induced. Focusing on the case of two AC grids interconnected with an HVDC link, the HVDC interconnector consists of two converter stations. One of the stations has to manage the active power flow, while the other station controls the DC bus voltage. When a grid-following control is implemented in the station that is controlling the DC bus voltage, the other station can be operating as grid-forming control to provide inertial support. However, if the DC bus is controlled by a grid-forming converter to bring an inertial effect, this may induce some instability issues.

By implementing the grid-forming control in both substations, the impact of inertial support on the frequency dynamics needs to be assessed. Till now, this topic has not been widely studied in the literature, except for some examples in [7], [10]. Author in [10], by implementing the VSM-based control in both stations have demonstrated that it is possible to stabilize the system. However, integrating the feature of DC voltage regulation requires a slower performance for the DC controller and possibly increased DC-side capacitive energy storage.

In this paper, two different control configurations are adapted to an HVDC interconnection. In the first configuration, one terminal is controlled with a grid-forming structure for providing virtual inertia, while the other terminal is controlled with a grid-following structure, which regulates the DC bus voltage. In the second configuration, both terminals are controlled with grid-forming structure. It is demonstrated that in the first configuration, the DC bus voltage is properly controlled and the grid-forming converter provides the inertial support. If the aim is to have a symmetrical inertial support, the second configuration is used. Therefore, the DC voltage control task is given to a grid-forming converter. In this case, it has been highlighted that there is a contradictory effect between the DC voltage regulation and inertial effect. Hence, a proper inertial effect cannot provided by the grid-forming converter that is responsible for the DC voltage control. To solve this issue and have a fully symmetrical behavior, it is proposed to integrate a flywheel energy storage system (FESS) connected with an additional converter to the DC link in order to control the DC voltage. As the result, an adequate performance on the DC voltage regulation as well as inertia provision at both HVDC substations are achieved. Finally, a method is proposed to have a basic idea about the sizing of the storage system.

II. RECALL ON GRID-FOLLOWING AND GRID-FORMING CONTROL STRUCTURES

Grid-following power converters are mainly designed to deliver power to an energized grid. They can be represented as an ideal current source connected to the grid in parallel with high impedance. The grid-following structure utilized in this paper is captured from [2]. An overview of this type control is presented in Fig. 1. A current control loop with a PI controller ($k_{pi} + k_{ii}/s$) regulates the converter current. A phase-locked-loop (PLL) block is used to synchronize the converter to the grid voltage at the PCC. It is supposed that the VSC is connected to the grid with a transformer, which is modeled with its series impedance $R_c + jX_c$. The grid is modeled by a Thevenin equivalent composed of a voltage source $v_{e_{abc}}$, an inductance L_g and a resistance R_g.

The grid-forming converters can be represented as an ideal AC voltage source with a low-output impedance. The grid-forming control structure used in this paper is based on the well-known VSM implementation [5]. An overview of this type control is illustrated in Fig. 2. To control the LC filter dynamics the voltage and current control loops are cascaded. The VSM implementation (right-hand side of Fig. 2) is based on a conventional swing equation representing the inertia H_{VSM} and damping coefficient k_d. The swing equation that is used for implementing the virtual inertia is determined by the power balance as follows:

$$2H_{VSM}.s.\omega_{VSM} = p^* - p + k_d(\tilde{\omega}_g - \omega_{VSM}), \quad (1)$$

where ω_{VSM} is the internal frequency and $\tilde{\omega}_g$ is the estimated grid frequency. As indicated in Fig.2, the frequency estimate is provided by a PLL.
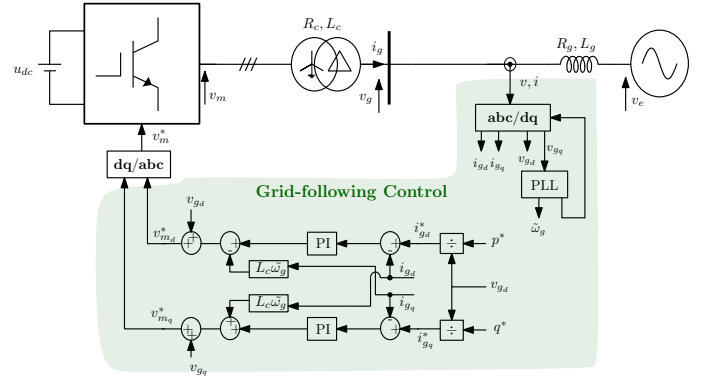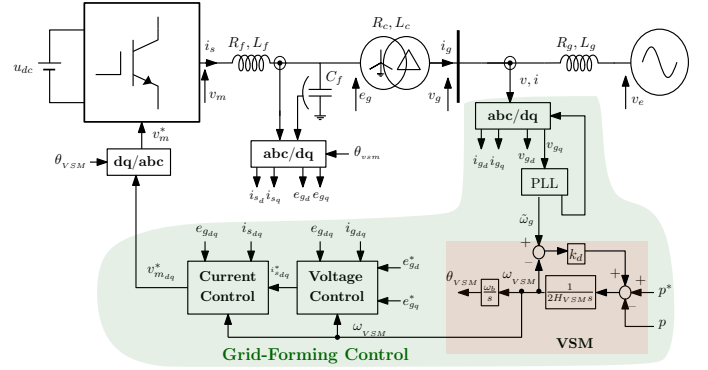

Fig. 1. Scheme of the grid-following control.

Fig. 2. Scheme of the VSM-based grid-forming control.

III. HVDC CONVERTER CONTROL IMPLEMENTATION

In order to investigate the impact of grid-forming control on the power system dynamics, two control system configurations of a point-to-point HVDC transmission system are presented. In the first configuration, one terminal is controlled with a grid-forming structure for providing virtual inertia, while the other terminal is controlled with a grid-following structure, which regulates the DC bus voltage. In the second configuration, both terminals are controlled with grid-forming structure trying to provide virtual inertia in both AC grids.

Fig. 3 presents an HVDC link with symmetric monopole topology interconnecting two AC grids. For the sake of simplicity, both AC grids are supposed to be identical. They are formed by a linear resistive load and an equivalent AC grid with a variable frequency. The equivalent AC grid consists of an inertial AC voltage source in series with its impedance, which is driven by a model representing the equivalent dynamic behavior of a large system. It consists of a swing equation and a lead-lag filter, which is a simplified model of the turbine dynamics [11]. A governor is added to support the grid frequency. p_g is the active power calculated from the grid side in per-unit. ω_e is the grid frequency. R is the droop control gain. H_{eq}, T_N and T_D are the inertia constant, the lead time constant and the lag time constant, respectively.

In the DC link, the charging time of the DC capacitors at each substation is considered to be 40 [ms] [9]. The DC cooper
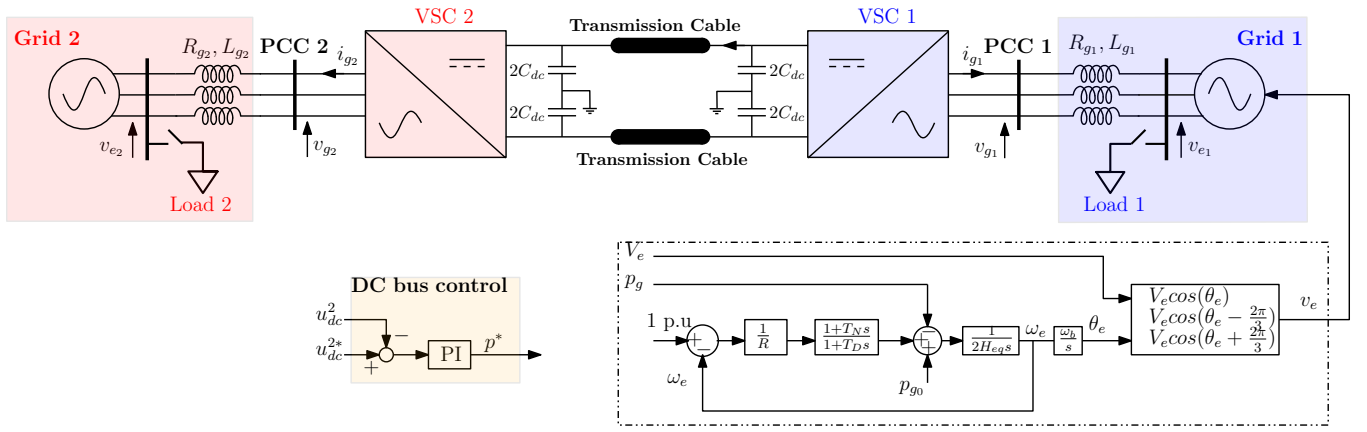
Fig. 3. Scheme of the HVDC interconnection.

TABLE I
SYSTEM AND CONTROL PARAMETERS

| AC grids			
$P_n = P_b = S_b$	1000 MW	$H_{eq1} = H_{eq2}$	5 s
$V_{b1} = V_{b2}$	320 kV	R	0.04 pu
$V_{e1} = V_{e2}$	1 pu	T_N	1 s
$L_g = 10R_g$	0.1 pu	T_D	2 s
ω_b	314.16 rad/s		
DC Bus			
u_{DC}	640 kV	L_{cable}	0.5 mH/km
C_{DC}	0.1953 mF	C_{cable}	8.6 nF/km
R_{cable}	0.02568 Ω/km	DC controller response time	100 ms
Grid-following converter			
L_c	0.15 pu	k_{ii}	171.9 pu
R_c	0.005 pu		
k_{pi}	0.568 pu	PLL response time	100 ms
Grid-forming converter			
L_c	0.15 pu	k_{pi}	0.73 pu
R_c	0.005 pu	k_{ii}	1.19 pu
C_f	0.066 pu	k_{pv}	0.52 pu
L_f	0.15 pu	k_{iv}	1.16 pu
R_f	0.005 pu	H_{VSM}	5 s
$e_{g_d}^*$	1 pu	k_d	202.6
$e_{g_q}^*$	0 pu	PLL response time	100 ms
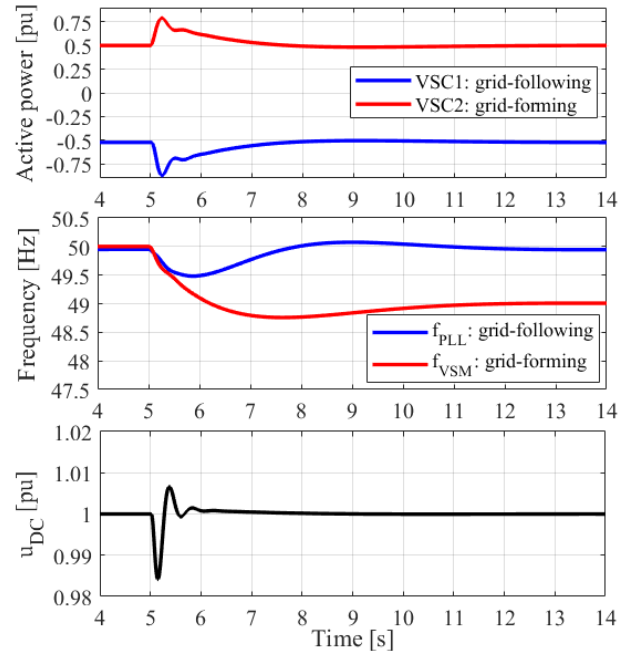
Fig. 4. Active power of VSCs, frequencies and DC bus voltage in case of load change in Grid 2.

cables with an area of 1000 [mm2], a total distance of 500 [km] is modeled with a PI connection (R_{cable}, L_{cable}, C_{cable}). Depending on the choice of the two previously mentioned configurations, the DC bus control is adapted to either grid-following VSC or grid-forming one to adjust their power references.

A. One Terminals Controlled as Grid-Following and the Other as Grid-Forming

It is assumed that the VSC1 is controlled as grid-following and it controls the DC bus voltage. VSC2 is controlled as VSM-based grid-forming. The control and system parameters are given in Table I.

Initially, 500 MW of power (0.5 p.u) is transferring from the Grid1 to Grid 2 ($P_{g1_0} = -P_{g2_0} = 0.5$ p.u) through the HVDC link. At $t = 5$ [s], a step of 500 MW is applied to the Load2 at Grid2 side. Fig. 4 shows the active power responses and

frequencies at VSC1 and VSC2 substations. It can be seen that the grid-forming VSC2 is participating to the frequency regulation thanks to its inertial response by injecting active power during transient. This transient power is absorbed from the Grid1 through VSC1. The DC bus voltage is also kept within an acceptable range (i.e. 0.95 p.u$\leq u_{DC} \leq$1.05 p.u) by VSC1's control.

In order to provide inertial support to Grid1 by the grid-following VSC1, a well-known approach is to derivate the Grid1 frequency estimated by the PLL and use this estimation in a separate loop to act on the power setpoint P_1^* [2]. Another option is to replace the grid-following VSC1 with a grid-forming converter that can provide the inertial support inherently. In any case, since the DC bus voltage control is also implemented to the VSC1 trying to regulate the DC voltage

by acting on P_1^*, it is worthy to investigate the performance of the VSC1 under these two simultaneous demands (i.e. inertial support and DC voltage control).

B. Two Terminals Controlled as Grid-Forming

In this subsection, the VSC1 is controlled as a VSM-based grid-forming converter in order to provide the inertial support to the Grid1. Simultaneously, this converter is controlling the DC bus voltage of the HVDC interconnection. Since the DC bus control is the outermost control loop, it should be slower than the power control loop to avoid interactions and possible instability. First, we keep the same DC bus control response time as before (i.e. 100 [ms]) and start with a small inertial constant in order to have a fast power control. Then, the inertia constant is increased as much as possible. It should be noted that by changing the value of inertia, the damping ratio of the VSM active power response is kept always to $\zeta = 0.7$ in our control tuning. Therefore, the damping term of the VSM (k_d) is updated with respect to the different choice of inertia constant.

Same as previously, 500 MW of power is transferring from the Grid1 to Grid 2 through the HVDC link. At $t = 5$ [s], a step of 500 MW is applied to the Load1 at Grid1 side. Fig. 5 shows the active power response of the VSC1 and DC bus voltage corresponding to this event. It can be seen that with $H_{VSM1} = 0.1$ [s], which is quite a small value and it results in a fast power control, the responses are well damped. If the aim is to provide the inertial support, a bigger inertia constant is needed. The results show that by increasing the inertia constant over 0.17 [s], there is a risk of instability due to the interaction between the power control loop and DC voltage control loop.

A primitive idea to solve this issue is to slowdown the DC bus regulation. Therefore, in the next simulation study presented in Fig. 6, the DC control response time is increased to 600 [ms]. From Fig. 6, it can be observed that with higher inertia constant, the response are well damped but with a larger deviation in the power and DC voltage. In fact, there is a fundamental conflict between the inertial support provision and DC bus voltage control. Focusing on the curves of active power and DC bus voltage, right after the disturbance, the VSC1 tends to inject power rapidly due to its inertial effect. At the same time, since the DC bus voltage is dropping, the DC voltage controller tries to reduce the power setpoint of VSC1 to maintain the DC bus level. Hence, these two actions introduce two opposite effects and neither the DC bus is controlled within the acceptable range nor a proper inertial support is provided. It can be seen that by choosing a bigger inertia constant, the frequency Nadir is not improved due to this contradiction.

To sum up, when asking for the DC bus voltage regulation and inertial support simultaneously from a single converter at an HVDC substation, two different conditions arise:

- If the DC voltage control loop is fast in order to achieve an adequate regulation of the DC voltage, the inertial effect must be very small in order to avoid the interactions
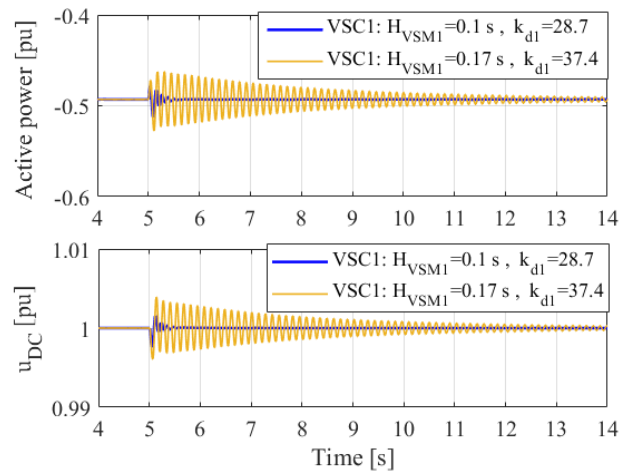

Fig. 5. Active power of VSC1 and DC bus voltage in case of load change in Grid1 considering a fast DC bus regulation.
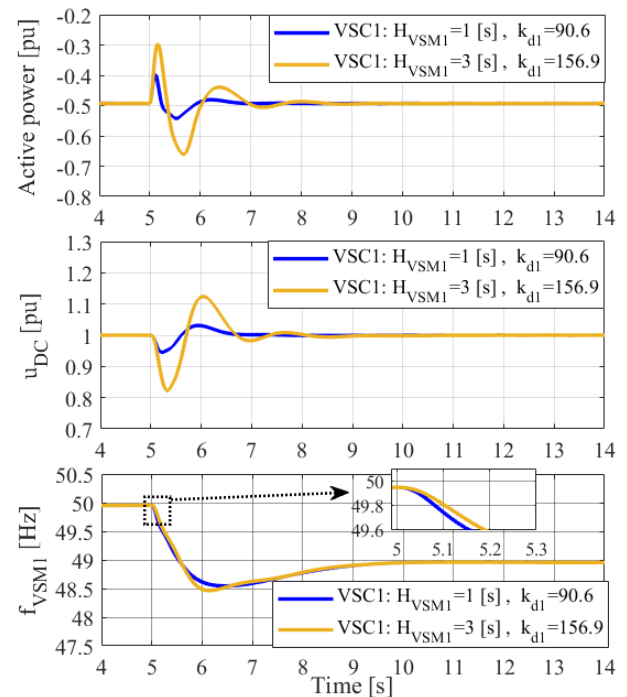

Fig. 6. Active power of VSC1, frequency and DC bus voltage in case of load change in Grid1 considering a slow DC bus regulation.

between the internal loop (power control loop) and the external one (DC voltage control loop).

- In order to be able to increase the inertia constant in power control loop, the DC voltage control loop has to be slower. In this case, the contradiction between the inertial support and DC voltage control prevents the DC voltage to be well-controlled and also to have a proper inertial effect.

The obtained results highlight the necessity of decoupling the DC voltage control task and the inertia provision. If the aim is to have an identical inertia support in both sides of an
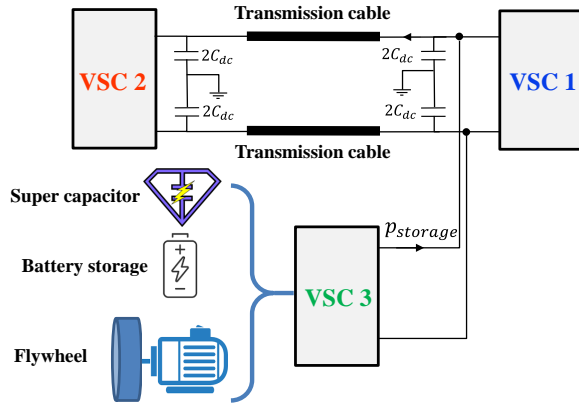
Fig. 7. Various energy storage systems that could be integrated to the DC bus of an HVDC interconnection.

Fig. 8. A simplified model of a FESS integrated to the DC bus of an HVDC interconnection.

HVDC interconnection (which is an essential need especially if the HVDC link connects two AC grids that belong to two different countries), the DC bus voltage needed be dynamically controlled with a third converter. In this case, the DC voltage control task is given to this new converter and two existing converters will provide the inertial support. Since the DC voltage is controlled by injecting/absorbing the active power to/from the DC link, an energy storage device is required to be integrated to the additional converter.

IV. INTEGRATION OF A STORAGE DEVICE TO THE DC BUS

There are different storage system technologies including super capacitor [12], battery energy storage system (BESS) [13] and flywheel energy storage system [FESS] [14] that can be used for this application (see Fig. 7). For the first two cases, a DC/DC step-up converter is needed to adapt the DC voltage levels. The FESS is considered as a rotating mass that stores some energy and it can be driven either by a permanent magnet synchronous generator (PMSM) or an induction machine (IM) [14]. Therefore, an AC/DC converter is essential to connect the FESS to the DC bus of an HVDC interconnection. It should be noted that the comparison of investment and operational costs for different storage systems (installed either in the DC link of an HVDC interconnection or in the AC side) is out of the scope of this paper. The main purpose is to highlight that an HVDC link with grid-forming control in both substations for the aim of inertia provision is facing physical challenges that could be solved by, for example, integrating a storage device to the DC bus.

In this paper, an FESS is used to support the DC bus of an HVDC interconnection, so that the two HVDC substation can take the required energy for the inertial support provision from the FESS. It should be mentioned that the main aim of this section is not evaluating the detailed modeling and control of an FESS, which has been widely studied in the literature [14]–[16], but giving an idea about how to size this kind of system. Hence, a simplified model of a rotating mass to derive an equivalent flywheel rotational speed is utilized.
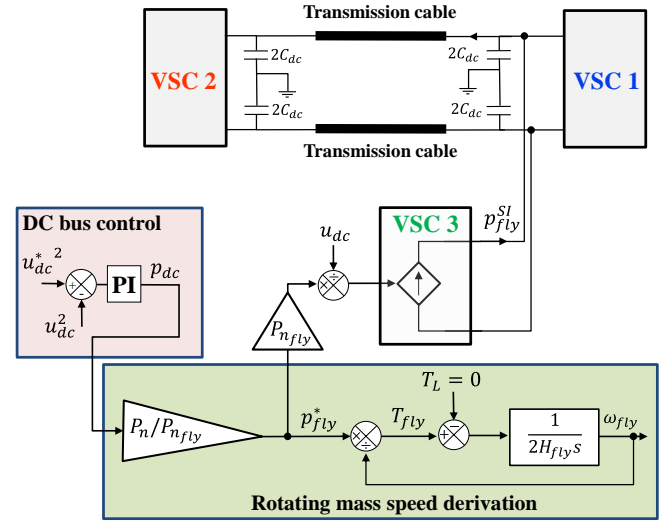
A. Simplified Model of an FESS

Considering that the required power to regulated the DC bus voltage is p_{dc} in per-unit, which is given by the DC voltage controller, the flywheel power reference p_{fly}^* is given by:

$$p_{fly}^* = p_{dc}.\frac{P_n}{P_{n_{fly}}}, \qquad (2)$$

where P_n and $P_{n_{fly}}$ are the nominal power of the HVDC interconnection and the FESS, respectively. The flywheel speed can be derived from the well-known swing equation:

$$T_{fly} - T_L = 2H_{fly}\frac{d(\omega_{fly})}{dt}, \qquad (3)$$

where $T_{fly} = p_{fly}^*/\omega_{fly}$ is the flywheel torque, T_L is the load torque that is considered to be zero and H_{fly} is the rotational inertia of the flywheel. Fig. 8 presents the simplified model of the FESS integrated to the HVDC interconnection.

B. Sizing of the Storage System

In order to have a proper control of the DC bus voltage, the AC power variation Δp at each substation needs to be well supported by the storage system. This means that, ideally, FESS has to be sized according to the maximum AC power variation ΔP_{max}. Focusing on the dynamic equation of the VSM-based control adopted to VSC1/VSC2 ($\Delta p^* = 0$):

$$\Delta\omega_{VSM} = \frac{1}{2H_{VSM}s + k_d}\left[-\Delta p + k_d\Delta\tilde{\omega}_g\right]. \qquad (4)$$

Based on the power/angle relation [6]:

$$\Delta p = K_c(\Delta\delta_{VSM} - \Delta\delta_g) = K_c\frac{\Delta\omega_{VSM} - \Delta\omega_g}{s}\omega_b, \qquad (5)$$

where $K_c = (E_g V_g)/X_c$ and δ_{VSM} and δ_g are the phasor angle of the modulated voltages e_g and PCC voltage v_g, respectively. Neglecting the dynamics of the PLL ($\Delta\omega_g = \Delta\tilde{\omega}_g$):

$$\Delta\tilde{\omega}_g = \Delta\omega_{VSM} - \frac{s\Delta p}{K_c\omega_b}. \qquad (6)$$

By substituting (6) in (4):

$$\Delta\omega_{VSM} = -\frac{1}{2H_{VSM}s}\left[1 + \frac{k_d s}{K_c\omega_b}\right]\Delta p. \qquad (7)$$

If the damping k_d is negligible:

$$\Delta p = -\frac{2H_{VSM}}{f_0}\frac{d(\Delta f_{VSM})}{dt}. \qquad (8)$$

The term $d(\Delta f_{VSM})/dt$ is known as the rate of change of frequency (RoCoF). Considering that the maximum RoCoF is an available information (e.g. by a transmission system operator (TSO)). For a given maximum RoCoF, the maximum power variation is obtained by:

$$\Delta P_{max} = -\frac{2H_{VSM}}{f_0}.RoCoF_{max}. \qquad (9)$$

ΔP_{max} determines the size of the FESS. If the damping term is not negligible:

$$\Delta P_{max} = -\frac{2H_{VSM}}{f_0}.RoCoF_{max} - \frac{2H_{VSM}k_d}{K_c\omega_b}\frac{d(\Delta p)}{dt}. \qquad (10)$$

Considering an AC load connection that causes a positive power variation during first few seconds of transient and a negative RoCoF, the first term of (10) is positive and its second term is negative. Therefore, the power variation is less than expected due to the damping term. The same analysis in case of an AC load shedding implies that the damping effect of the VSM reduces the injected power corresponds to a given RoCoF in transient. Therefore, the sizing of the FESS according to (9) induces a bit of oversizing depending on the tuning of the VSM-based grid-forming converter at each HVDC substation.

As an illustrative example, assuming that $RoCoF_{max} = -2$ [Hz/s], and $H_{VSM} = 5$ [s], then according to (9) the maximum power variation is $\Delta P_{max} = 0.4$ p.u. Therefore, the FESS is sized to the same value ($P_{n_{fly}} = 400$ [MW]). The flywheel inertia is $H_{fly} = 5$ [s]. In the simulation environment, initially, 500 MW of power is transferring from the Grid1 to Grid 2. A step of 500 MW is applied to the Load 2 at $t = 5$ [s]. The damping ratio of the both VSM-base grid-forming converters is $\zeta = 0.7$. The results of this case study are given in Fig. 9. It can be seen that the maximum power variation of VSC2 is less than the theoretical value due to the damping effect. The flywheel supports the DC bus voltage properly and it is a good buffer to avoid propagation of the disturbance to the Grid1.The flywheel's maximum transient power is higher than
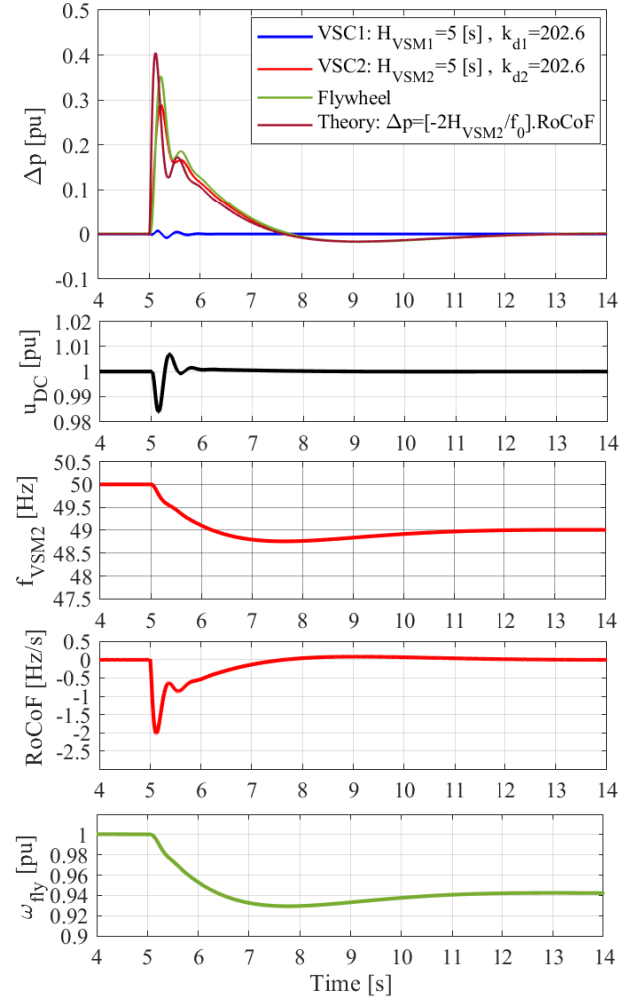

Fig. 9. Responses to the load disturbance in Grid2 considering the damping ratio of $\zeta = 0.7$ for both substations.
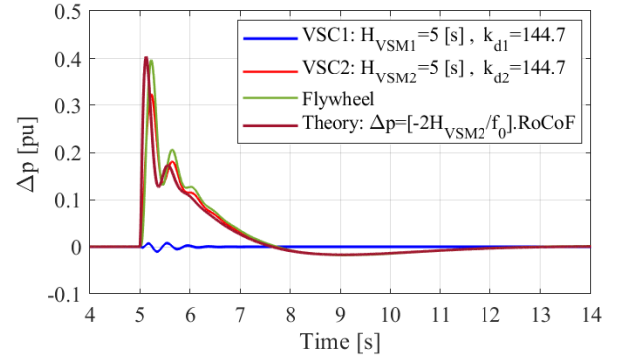

Fig. 10. Responses to the load disturbance in Grid2 considering the damping ratio of $\zeta = 0.5$ for both substations.

the VSC2. This is due to a delay induced by the DC control response time. It is noted that the maximum power provided by the FESS is slightly less than the expected theoretical value.

In order to see the impact of damping on the proposed sizing of the FESS, the same study as previously is performed with a low damping ratio of $\zeta = 0.5$ at each substation. In this case,

as shown in Fig. 10, the peak power of VSC2 and accordingly the FESS are increased. However, the FESS maximum transient power is still slightly less that the theoretical value. The obtained results highpoint the proposed simple idea to size the FESS integrated to an HVDC interconnection based on a given maximum RoCoF.

It should be mentioned that in previous example, where the inertia support provided by HVDC substations was based on $H_{VSM} = 5$ [s], the calculated size of the FESS was quite large (0.4 p.u). If the HVDC owner tends to utilize a smaller storage system for inertia provision, the maximum transient AC power needs to be reduced and this can be done by reducing the inertia constant of the substations. As an example, assuming: $RoCoF_{max} = -2$ [Hz/s], and $H_{VSM} = 2.5$ [s], then according to (9) the maximum power variation is $\Delta P_{max} = 0.2$ p.u. Therefore, the FESS is sized to the same value ($P_{n_{fly}} = 200$ [MW]). Considering $H_{fly} = 2.5$ [s], in the simulation environment, initially, 500 MW of power is transferring from the Grid1 to Grid 2. A step of 400 MW is applied to the Load 1 at $t = 5$ [s] in order to achieve $RoCoF_{max} = -2$ [Hz/s]. The damping ratio of the both VSM-base grid-forming converters is $\zeta = 0.7$. The results of this case study are given in Fig. 11. It can be seen that the maximum power variation of the flywheel with reduced size is closed to the theoretical size, which confirms, again, the proposed simplified sizing approach.

V. CONCLUSIONS

In this paper, the inertia provision by an HVDC interconnection was evaluated. It was demonstrated that by controlling one HVDC substation with grid-following converter that controls the DC bus voltage and the controlling the other substation with grid-forming control that manages the power flow through the HVDC link, it is possible to have a proper inertial effect in the grid-forming side. However, if the aim is to have an identical inertial support at both substations, there is a conflicting effect between the inertia emulation and the DC bus control. In this case, it was shown that neither the DC link is controlled very well nor a proper inertial support is provided. To solve this issue, it was proposed to integrate an FESS to the HVDC link in order to control the DC bus voltage so that the two substations can provide the inertial support straightforwardly. Finally, a simplified approach to size the FESS was proposed.

ACKNOWLEDGMENT

REFERENCES

[1] A. Ulbig, T. S. Borsche, and G. Andersson, "Impact of low rotational inertia on power system stability and operation," in *19th IFAC World Congress*, 2014, pp. 7290–7297.
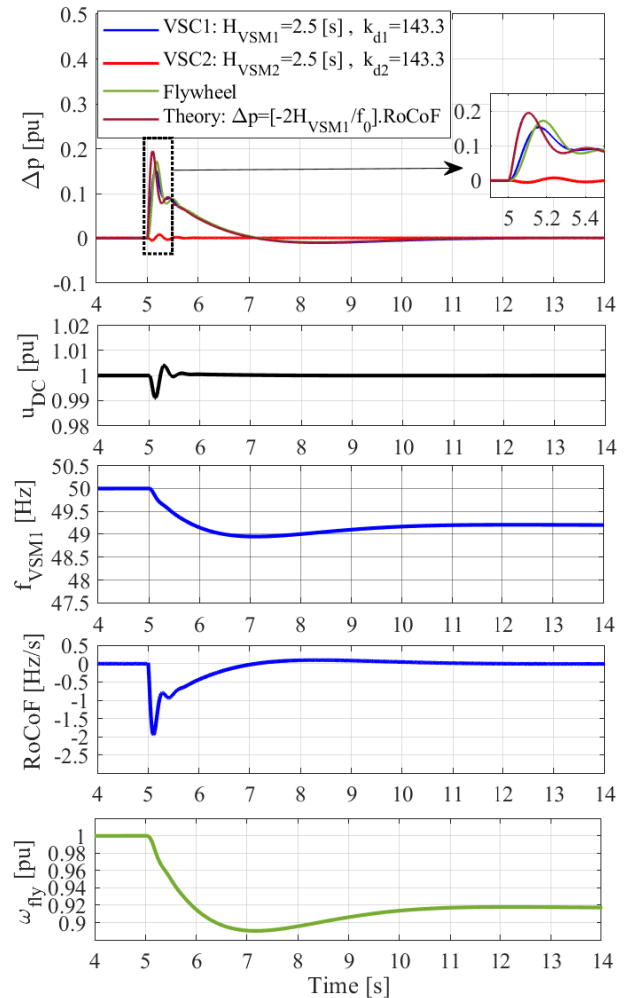

Fig. 11. Responses to the load disturbance in Grid1 considering a reduced size of the FESS.

[2] J. Zhu, C. D. Booth, G. P. Adam, A. J. Roscoe, and C. G. Bright, "Inertia emulation control strategy for VSC-HVDC transmission systems," *IEEE Trans. Power Syst.*, vol. 28, no. 2, pp. 1277–1287, 2013.

[3] E. Rakhshani and P. Rodriguez, "Inertia Emulation in AC/DC Interconnected Power Systems Using Derivative Technique Considering Frequency Measurement Effects," *IEEE Trans. Power Syst.*, vol. 32, no. 5, pp. 3338–3351, Sep. 2017.

[4] E. Rokrok, T. Qoria, A. Bruyere, B. Francois, and X. Guillaud, "Effect of Using PLL-Based Grid-Forming Control on Active Power Dynamics Under Various SCR," in *IECON 45th Annual Conference of the IEEE Industrial Electronics Society*, 2019. [Online]. Available: https://sam.ensam.eu/handle/10985/16655. [Accessed: 27-Sep-2019].

[5] S. D'Arco, J. A. Suul, and O. B. Fosso, "A Virtual Synchronous Machine implementation for distributed control of power converters in SmartGrids," *Electr. Power Syst. Res.*, vol. 122, pp. 180–197, 2015.

[6] T. Qoria, E. Rokrok, A. Bruyere, B. Francois, and X. Guillaud, "A PLL-Free Grid-Forming Control with Decoupled Functionalities for High-Power Transmission System Applications," *IEEE Access*, vol. 8, pp. 197363–197378, Oct. 2020.

[7] R. Aouini, B. Marinescu, K. Ben Kilani, and M. Elleuch, "Synchronverter-Based Emulation and Control of HVDC Transmission," *EEE Trans. Power Syst.*, vol. 31, no. 1, pp. 278–286, Jan. 2016.

[8] M. Guan, W. Pan, J. Zhang, Q. Hao, J. Cheng, and X. Zheng, "Synchronous Generator Emulation Control Strategy for Voltage Source Converter (VSC) Stations," in *IEEE Trans. Power Syst.*, vol. 30, no. 6, pp. 3093–3101, Nov. 2015.

[9] E. Rokrok, T. Qoria, A. Bruyere, B. Francois, and X. Guillaud, "Clas-

sification and dynamic assessment of droop-based grid-forming control schemes: Application in HVDC systems," *Electr. Power Syst. Res.*, vol. 189, p. 106765, Dec. 2020.

[10] F. Palombi, L. Piegari, S. D'Arco, A. G. Endegnanew, and J. A. Suul, "Impact on Power System Frequency Dynamics from an HVDC Transmission System With Converter Stations Controlled as Virtual Synchronous Machines," in *2019 IEEE Milan PowerTech*, 2019, pp. 1–6.

[11] T. Qoria, F. Gruson, F. Colas, G. Denis, T. Prevost, and X. Guillaud, "Inertia effect and load sharing capability of grid forming converters connected to a transmission grid," in *15th IET International Conference on AC and DC Power Transmission (ACDC 2019)*, 2019.

[12] M. Farhadi and O. Mohammed, "Energy Storage Technologies for High-Power Applications," *IEEE Trans. Ind. Appl.*, vol. 52, no. 3, pp. 1953–1962, May 2016.

[13] J. Guo, D. Jiang, Y. Zhou, P. Hu, Z. Lin, and Y. Liang, "Energy storable VSC-HVDC system based on modular multilevel converter," *Int. J. Electr. Power Energy Syst.*, vol. 78, pp. 269–276, Jun. 2016.

[14] M. I. Daoud, A. M. Massoud, A. S. Abdel-Khalik, A. Elserougi, and S. Ahmed, "A Flywheel Energy Storage System for Fault Ride Through Support of Grid-Connected VSC HVDC-Based Offshore Wind Farms," *IEEE Trans. Power Syst.*, vol. 31, no. 3, pp. 1671–1680, May 2016.

[15] F. Díaz-González, A. Sumper, O. Gomis-Bellmunt, and F. D. Bianchi, "Energy management of flywheel-based energy storage device for wind power smoothing," *Appl. Energy*, vol. 110, pp. 207–219, 2013.

[16] G. Cimuca, S. Breban, M. M. Radulescu, C. Saudemont, and B. Robyns, "Design and control strategies of an induction-machine-based flywheel energy storage system associated to a variable-speed wind generator," *IEEE Trans. Energy Convers.*, vol. 25, no. 2, pp. 526–534, 2010.